

Effect of Surface Geometry on Polymer Adsorption. 2.[†] Individual Adsorption and Competitive Adsorption

Masami Kawaguchi,* Sachio Anada, Koh-ichi Nishikawa, and
Nobuhiro Kurata

Department of Chemistry for Materials, Faculty of Engineering, Mie University,
1515 Kamihama-cho, Tsu, Mie 514, Japan

Received August 23, 1991; Revised Manuscript Received November 20, 1991

ABSTRACT: Kinetics and isotherms of individual and binary mixtures of various polystyrenes (PS) with narrow molecular weight distributions on three porous silica surfaces have been investigated in cyclohexane and in carbon tetrachloride as a function of the ratio of the pore size to twice the radius of gyration of a PS chain in a bulk solution. Adsorption isotherms of the individual PS chains are of the high affinity type. When the size ratio is less than 2, the adsorbed amounts obtained at the plateau of the adsorption isotherms are less than those for the nonporous silica and decrease with a decrease in the size ratio. The rate at which PS chains attain equilibrium for the large pore ratio is much faster than that for the small one. The adsorbed amount is linear in the square root of time for the initial stage of the adsorption, suggesting that the initial stage is dominated by a diffusion process. The effect of solvent power on kinetics is more pronounced at higher initial concentrations. For the competitive adsorption, when both PS chains can penetrate easily into the pores, the shape of the adsorption isotherm resembles the high affinity type and the large PS adsorbs preferentially. By contrast, when the small PS adsorbs more than the large PS for the individual adsorption, the adsorption isotherm has a rounded shape.

Introduction

Polymer adsorption phenomena have been studied intensively to gain understanding of the interaction between polymer chains and an adsorbent and of the interfacial properties of adsorbed polymer chains such as their conformations. They are also fundamentally related to the practical applications of chromatography, painting, adhesion, coatings, suspensions, flocculation, dispersion, etc. The theoretical and experimental studies of this subject have been reviewed.¹⁻⁵ Most studies have focused on polymer adsorption at equilibrium. By contrast, the kinetics of polymer adsorption are poorly understood.

In general, the process of polymer adsorption is roughly classified into the following three stages: (1) diffusion to the surface; (2) the conformational changes required to relax the polymer toward its equilibrium conformation; and (3) effects of other polymer molecules which may displace segments initially adsorbed. However, there are no theoretical guidelines for the adsorption kinetics. For a flat and smooth surface, ellipsometry is a valuable technique for rate studies and it gives both the adsorbed amount and the layer thickness. Results for polystyrenes on metal surfaces showed that the two measured quantities did not stay in step: the layer thickness attained its plateau value in 200-300 min, while the adsorbed amount reached its plateau value in 1 day.⁶⁻⁸ Some techniques were used to investigate the polymer adsorption kinetics, and several kinetic models have been proposed.⁹⁻¹⁵

Adsorption to a heterogeneous and porous surface should be more complex than that to a flat and smooth surface, and the time to attain equilibrium for porous surfaces may be much longer than that for flat surfaces. The polymer adsorption to a heterogeneous surface should be an important area of investigation, since in many applied colloidal systems highly irregular particles have to be used. There have been few attempts to systematically study surface geometry effects on polymer adsorption in terms of isotherms and kinetics of the individual and competitive

adsorptions. Furusawa, Yamashita, and Konno have reported the competitive adsorption of polystyrenes onto porous silicas in cyclohexane (a θ solvent).¹⁶ However, they did not deeply discuss the surface geometry effect on the competitive adsorption.

In this paper, we examine kinetics and adsorption isotherms for individual and competitive adsorptions of polystyrenes with narrow molecular weight distributions on well-defined porous silica surfaces with relatively narrow pore distributions as a function of the ratio of the pore size to twice the radius of gyration of a polystyrene in a bulk solution and as a function of solvent power. Moreover, we compare these experiments with the results of Furusawa et al.¹⁶ to explain how this work differs from theirs.

Experimental Section

Materials. Six polystyrenes (PS) with narrow molecular weight distributions, having $M_w = 9.0 \times 10^3$ (PS-9), 37.9×10^3 (PS-38), 96.4×10^3 (PS-96), 355×10^3 (PS-355), 706×10^3 (PS-706), and 1260×10^3 (PS-1260) were purchased from Tosoh Co. The polydispersities of PS-9, PS-38, PS-96, PS-355, PS-706, and PS-1260 were determined to be 1.05, 1.01, 1.01, 1.02, 1.05, and 1.05, respectively, using a Toyo Soda HLC-802 A gel permeation chromatography instrument with UV-8 Model II detection. The wavelength used was 254 nm. The eluent solvent used was tetrahydrofuran.

Carbon tetrachloride was distilled before use. Cyclohexane and dioxane were of spectrograde quality and were used without further purification.

The adsorbents used were three porous micro bead (100-200 mesh) silica gels (MB-300, MB-800, and MB-1300; Fuji-David Chemical Co., Japan). The surface area (S) and the average pore diameter (d) were determined from N_2 adsorption and a mercury porosimeter, respectively. The latter method characterizes the pore size distributions. From the pore size distributions, we characterized the breadth and skewness of the distributions by D90 and D10: 90% of the pore diameters are larger than the value of D90 and 10% are larger than that of D10. Characteristics of the respective silica surfaces are summarized in Table I.

The silica particles were purified by washing with hot carbon tetrachloride using a Soxhlet apparatus for 3 days. The purified silicas were dried in a desiccator under vacuum using an aspirator and further dried in a vacuum oven at 130-150 °C for several

[†] Part 1: Reference 17.

Table I
Characteristics for Silica Surfaces

silica	$S, \text{m}^2/\text{g}$	d, nm	D90, nm	D10, nm
MB-300	118	28.5	23	44
MB-800	45	81.3	75	112
MB-1300	27	129.9	122	174

days. The silica particles were kept in the vacuum oven to prevent contamination at room temperature before use. The purification method of the porous silicas was almost the same as that described in our previous paper.¹⁷

Adsorption of PS. PS was dissolved in carbon tetrachloride or in cyclohexane to desired concentrations. A fixed amount of silica was transferred to a 50-mL flask to maintain a similar surface area for the respective silica particles (0.15 g for MB-300, 0.40 g for MB-800, and 0.67 g for MB-1300) and then mixed with 10 mL of solvent. The sample was placed in an air incubator for 24 h at 35 °C to allow the solvent to fully penetrate into the pores. It was then mixed with 10 mL of PS solution. The mixture in the glass flask was mechanically shaken at a constant speed, usually 100 rpm in a Yamato BT-23 water incubator attached with a shaker for 24 h to determine adsorption isotherms. For adsorption kinetic studies the supernatant was carefully withdrawn after a fixed time interval.

The adsorbed amounts of PS were determined from the difference in the concentrations between the dosage (C_0) and the supernatant (C_p) and from the added silica amount. The value of C_p was determined as follows: after the evaporation of the solvent, the residue was dried in a vacuum oven at room temperature for 24 h and then dissolved in a fixed amount of dioxane using an Ohstuka Denshi System 77 UV spectrometer to measure the C_p . The intensities of the dioxane solutions were measured at $\lambda = 266 \text{ nm}$, where the extinction coefficient was $76.5 \text{ L mol}^{-1} \text{ cm}^{-1}$. There were two reasons why we took such a complex procedure to determine the C_p : Carbon tetrachloride interferes in a UV measurement, and there is the possibility that a cyclohexane PS solution would be turbid at ambient temperature since its θ point is 35 °C.

Competitive adsorption experiments in carbon tetrachloride were performed on a 1:1 (w/w) mixture of PS-96 and PS-355 using a procedure similar to that in the individual adsorption. After evaporation of carbon tetrachloride, the two residues of each system investigated were dissolved in a definite amount of dioxane and tetrahydrofuran, respectively. The dioxane solution was analyzed by UV spectroscopy to determine the total adsorbed amount, whereas the tetrahydrofuran solution was analyzed by gel chromatography to determine the adsorbed amounts of the respective PS samples.

For kinetic studies of the competitive adsorption of the 1:1 (w/w) mixture, after a fixed time interval supernatant was carefully withdrawn. Determination of the composition of the supernatant was carried out as described above. For all experiments the temperature of the water in the incubator was controlled to 35 ± 0.1 °C.

To confirm the reproducibility of the experiments, we performed at least two measurements for each concentration. The error in the adsorbed amount was less than 5%. Hereafter, the size ratio is defined as the ratio of the average pore diameter to twice the radius of gyration of a PS chain in the solvent.

Results and Discussion

Kinetics of Individual Adsorption. To calculate the size ratios, we estimate the radius of gyration ($\langle R^2 \rangle^{1/2}$), which was calculated from the relation between the radius of gyration and the molecular weight determined by Berry¹⁸ in cyclohexane, whereas in carbon tetrachloride it was determined from the intrinsic viscosity in the solvent at 35 °C, determined with a Ubbelohde viscometer, and the Flory-Fox relation. Typical viscosities and calculated $2\langle R^2 \rangle^{1/2}$ values for PS chains are summarized in Table II.

Figure 1 shows plots of the adsorbed amounts, A , of PS-38 for the MB-300, MB-800, and MB-1300 silicas at the initial PS concentration, $C_0 = 0.02 \text{ g}/100 \text{ mL}$ in carbon

Table II
Molecular Characteristics of PB Chains

$M_w \times 10^{-3}$	$2\langle R^2 \rangle^{1/2} \text{ in cyclohexane, nm}$	$2\langle R^2 \rangle^{1/2} \text{ in CCl}_4, \text{ nm}$	$[\eta] \text{ in CCl}_4, 100 \text{ mL/g}$
37.9	10.7	13.8	0.27
96.4	17.1	23.4	0.51
355	32.9	48.8	1.26
706	46.3	71.2	1.97

^a Calculated from Berry's relation, $\langle R^2 \rangle = 7.6 \times 10^{-18} M_w$. ^b Calculated from $[\eta] = 3.09 \times 10^{22} \langle R^2 \rangle^{3/2} / M_w$.

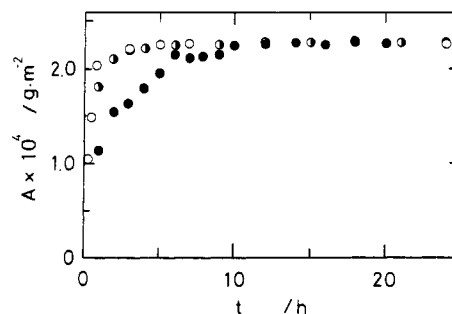


Figure 1. Adsorbed amounts, A , of PS-38 for porous silicas as a function of adsorption time, t , at $C_0 = 0.02 \text{ g}/100 \text{ mL}$ in carbon tetrachloride: MB-300 (●); MB-800 (○); MB-1300 (□).

tetrachloride as a function of adsorption time. Since twice the radius of gyration of the PS-38 estimated as 13.8 nm is smaller than the average pore size of the three silicas, the PS-38 molecules can easily penetrate into the pores without significant deformation of the PS chains and then they should be adsorbed onto the pore wall. The PS-38 chains adsorb faster on the surfaces of MB-800 and MB-1300 than on that of MB-300 (Figure 1); the adsorption time required to attain the plateau of $\text{ca. } 2.2 \times 10^{-4} \text{ g/m}^2$, which corresponds to the adsorption of all PS-38 molecules, is less than 5 h for MB-800 and MB-1300, while it is 10 h for MB-300. This difference correlates with the size ratios, which are 2.06, 5.87, and 9.39 for MB-300, MB-800, and MB-1300, respectively.

It is interesting to study the effect of solvent power on adsorption kinetics as a function of the size ratio. Cyclohexane is a θ solvent, and carbon tetrachloride is a good solvent for PS. From Table II, the $2\langle R^2 \rangle^{1/2}$ values of the PS-355 chain in cyclohexane and in carbon tetrachloride are larger than the average pore size in MB-300. Thus, the effective adsorption area for the PS-355 molecules should be reduced. The PS-355 molecules have to be distorted to become accessible to the pore inside MB-300. In contrast to MB-300, the pore sizes in both MB-800 and MB-1300 are clearly larger than the $2\langle R^2 \rangle^{1/2}$ value of the PS-355 chain in both solvents. As expected, the adsorption rates of PS-355 for the three silica surfaces at $C_0 = 0.02 \text{ g}/100 \text{ mL}$ in cyclohexane and in carbon tetrachloride strongly depend on the silica as shown in Figure 2.

All PS-355 molecules for the MB-800 and MB-1300 silicas adsorb in 24 h, but the adsorption processes are very different. The adsorbed amount for MB-1300 quickly establishes its plateau value in 5 h due to the large size ratio. The adsorption process for MB-800 is complex, and there are two apparent plateau regions. During the initial stage of the 5-h interval, over 60% of the dosage is adsorbed. For the middle adsorption time from 5 to 12 h the adsorbed amounts are almost constant, and then they gradually attain a plateau value. As mentioned above, this plateau value corresponds to true equilibrium. A similar adsorption process with the middle plateau stage is also observed for the PS-38-MB-300 pair as shown in

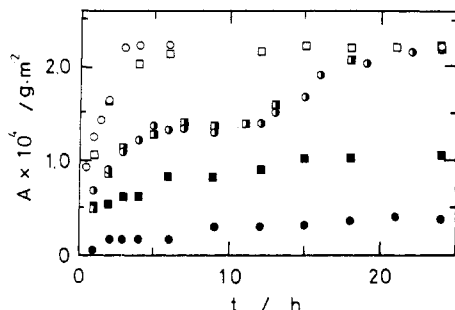


Figure 2. Adsorbed amounts, A , of PS-355 for porous silicas as a function of adsorption time, t , at $C_0 = 0.02$ g/100 mL in cyclohexane and carbon tetrachloride: MB-300 in cyclohexane (■) and carbon tetrachloride (●); MB-800 in cyclohexane (□) and carbon tetrachloride (○); MB-1300 in cyclohexane (□) and carbon tetrachloride (○).

Figure 1, but the middle adsorption time is relatively short. This is attributed to the difference in the size ratio between the PS-38-MB-300 pair (2.06) and the PS-355-MB-800 pair (1.67).

However, the effect of the solvent power on adsorption kinetics of PS-355 on the MB-800 and MB-1300 silicas is not clearly observed. The similar trend in both solvents can be interpreted by taking into account the difference in the segmental adsorption energy between these solvents. This energy can be estimated from the displacement adsorption^{17,19-23} of the adsorbed polymer chains by the addition of the displacer molecules using the theory of Cohen Stuart, Fleer, and Scheutjens.²⁰ Recently, Van der Beek, Cohen Stuart, Fleer, and Hofman determined segmental adsorption energies for PS on silica of 1.0 and 1.9 kT , from carbon tetrachloride and from cyclohexane, respectively.²³ This result leads to the conclusion that PS chains adsorb more strongly on a silica surface from cyclohexane than from carbon tetrachloride solution and PS chains are harder to desorb from the former solvent. Therefore, in cyclohexane the slower conformational changes of adsorbed PS chains within the pores may be compensated by the large size ratio. As a result, similar adsorption kinetics are observed in both solvents.

For the MB-300 silica in carbon tetrachloride the PS-355 molecules (size ratio = 0.58) were gradually adsorbed with an increase in the adsorption time with two steps and finally attained a plateau of 0.3×10^{-4} g/m². Reduction of the solvent power leads to a larger adsorption at equilibrium, but the kinetic behavior is similar to that in carbon tetrachloride.

Next, we focused on the effect of the polymer concentration on adsorption kinetics. In Figure 3, the adsorbed amounts of the PS-706 on MB-1300 at two concentrations are shown as a function of adsorption time. Their size ratios are 2.81 and 1.82 in cyclohexane and in carbon tetrachloride, respectively. Therefore, PS-706 chains can less easily penetrate into the pores in MB-1300. Though data points at the low concentration are somewhat scattered, the adsorption kinetics in both solvents are similar and most of PS chains adsorb in 24 h. In contrast with the low concentration, at the high concentration the kinetics are different and adsorption increases in the initial stage more steeply in cyclohexane than in carbon tetrachloride. The amount adsorbed at equilibrium from cyclohexane is 2.5 times larger than that from carbon tetrachloride. The time for attaining equilibrium is not very different between the two solvents. A similar kinetic behavior was observed for the PS-355-MB-800 pair at $C_0 = 0.2$ g/100 mL where the adsorbed amount is well in the plateau region and

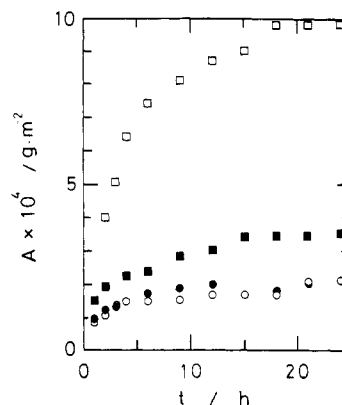


Figure 3. Adsorbed amounts, A , of PS-706 for MB-1300 at different C_0 as a function of adsorption time, t , in cyclohexane and carbon tetrachloride: at $C_0 = 0.02$ g/100 mL in cyclohexane (○) and carbon tetrachloride (●); at $C_0 = 0.1$ g/100 mL in cyclohexane (□) and carbon tetrachloride (■).

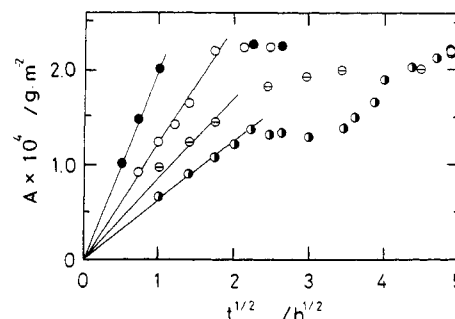


Figure 4. Plots of the adsorbed amounts, A , of various PS at $C_0 = 0.02$ g/100 mL in carbon tetrachloride vs the square root of adsorption time, t : PS-38-MB-1300 (●); PS-355-MB-1300 (○); PS-706-MB-1300 (□); PS-355-MB-800 (◇).

their size ratios are 2.47 and 1.67 in cyclohexane and in carbon tetrachloride, respectively (not shown here).

Returning to the initial stage of the adsorption process, if the adsorption is controlled by the diffusion of PS chains, a linear dependence of the adsorbed amount, A , on the square root of the time, t , would be expected;^{9,10} i.e.

$$A \sim t^{1/2} \quad (1)$$

We plotted the adsorbed amount versus the square root of the adsorption time. Typical plots are displayed in Figure 4, where all PS chains almost adsorb in 24 h at $C_0 = 0.02$ g/100 mL. They are all linear for the first 5 h, though the data points are somewhat scattered. The initial slope of the square root plot increases with an increase in the size ratio. Thus, the initial stage is considered to be mainly governed by polymer diffusion into porous materials. The term "diffusion" used here refers to an over-constrained diffusion, an adsorption of polymer chains accompanied by conformational changes. If the diffusion coefficient for such a complex process is obtained, its magnitude is much smaller than the diffusion coefficient in a bulk solution.

On the other hand, polymer diffusion in porous materials without polymer adsorption has been extensively studied by gel permeation chromatography (GPC). The historical success of GPC has been reviewed in detail by Glöckner.²⁴ Recently, Bishop, Langley, and Karasz^{25,26} have investigated the diffusion of linear PS in porous silica by the technique of dynamic light scattering. They showed that the decreasing ratio of the diffusion coefficients in pores and in bulk, respectively, with an increase in the ratio of the size of the polymer relative to that of the pore is in

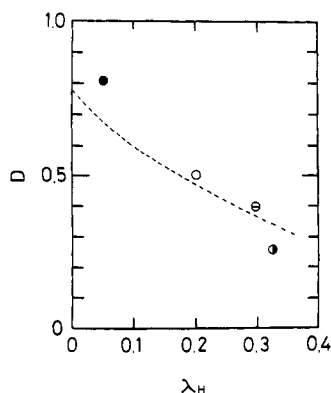


Figure 5. Plots of the reduced slope, D , as a function of the value of λ_H . The symbols are the same as in Figure 4. The dashed line indicates the ratio of the macroscopic diffusion coefficient of a PS chain in porous silica to the diffusion coefficient in a bulk solution.²⁵

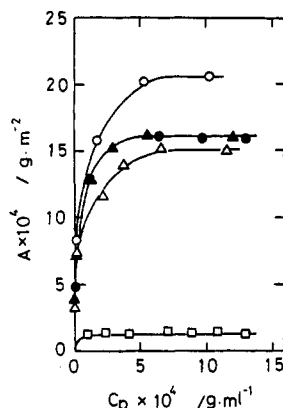


Figure 6. Adsorption isotherms of PS-38 and PS-355 on various silica surfaces in cyclohexane: PS-38-MB-800 (●); PS-38-MB-1300 (▲); PS-355-MB-300 (□); PS-355-MB-800 (▲); PS-355-MB-1300 (○).

good agreement with models for the diffusion of hard spheres in isolated cylindrical pores. Their study is not always consistent with this study since no polymer adsorption occurred in their study.

We made an attempt to analyze the data in Figure 4 by analogy to the analysis of macroscopic diffusion coefficients.²⁷ Figure 5 displays the reduced slopes, D , as a function of the parameter λ_H , the ratio of the hydrodynamic radius of PS to the pore radius. The D value is obtained as the ratio of the slope ($A/t^{1/2}$) for the plots in Figure 4 to a value of ($A/t^{1/2}$)₀ extrapolated to $\lambda_H = 0$ in the plot of $A/t^{1/2}$ versus λ_H . The hydrodynamic radius of PS was calculated from the relationship of the hydrodynamic radius and the radius of gyration.²⁸ In Figure 5, the data of Bishop et al. for the ratio of the macroscopic diffusion coefficient of a PS chain in porous silica to the diffusion coefficient in a bulk solution are compared and both values show a similar trend.

Isotherms of Individual Adsorption. Figures 6 and 7 display typical adsorption isotherms presented as the adsorbed amount (A) of PS chains versus C_p in cyclohexane and in carbon tetrachloride, respectively. Since the adsorbed amounts in 24 h were unchanged after 2 days, it can be assumed that 24 h is sufficient to attain true equilibrium, irrespective of silica, C_o , PS molecular weight, and solvent power. All adsorption isotherms correspond to the affinity type.

From Figure 6, the adsorption isotherm of PS-38 is almost independent of the silicas since the size of PS-38

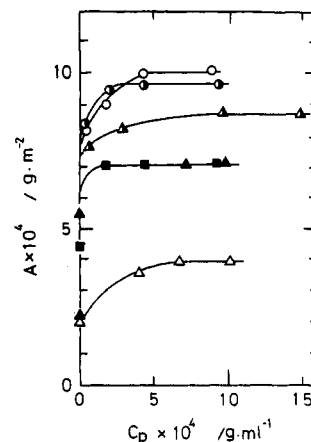


Figure 7. Adsorption isotherms of PS-38, PS-96, and PS-355 on various silica surfaces in carbon tetrachloride: PS-38-MB-300 (■); PS-38-MB-800 (▲); PS-96-MB-800 (▲); PS-96-MB-1300 (○); PS-355-MB-800 (▲); PS-355-MB-1300 (○).

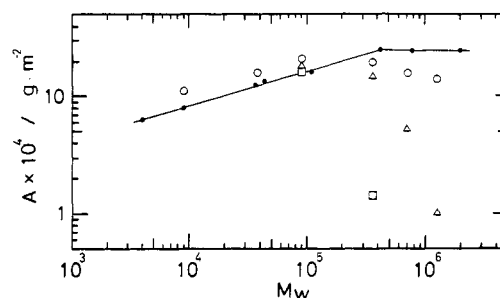


Figure 8. Double-logarithmic plots of the amounts adsorbed at the plateau in cyclohexane at various silica surfaces against the weight-average molecular weight: MB-300 (□); MB-800 (Δ); MB-1300 (○); Aerosil 130 (●). Since the respective amounts adsorbed for PS-9 and PS-38 are almost independent of the silica surface, the data are represented by the symbol O for MB-1300.

is much smaller than the average pore size for the porous silicas as mentioned in kinetic studies. Thus, it seems that all pores are available for adsorption of PS-38 regardless of the somewhat wide pore size distribution for the porous silicas. In contrast with PS-38, the adsorption isotherm of PS-355 depends strongly on the silica surfaces and the amount adsorbed at the plateau increases with an increase in the average pore size. In particular, the adsorbed amount for MB-300 is much less than that for MB-800 and MB-1300. This is due to the fact that the molecular size of PS-355 is larger than the pore size but smaller than that in MB-800 and MB-1300.

From Figure 7, the adsorption isotherm of PS-38 is the same, irrespective of the silica, and then the surface areas of the respective silicas are effectively used for adsorption of PS-38. By contrast with PS-38, the amounts adsorbed at the plateau for PS-96 and PS-355 increase with an increase in the average pore size.

In Figures 8 and 9, the amounts adsorbed at the plateau for PS and various silica surfaces are plotted double-logarithmically against the molecular weight in cyclohexane and in carbon tetrachloride, respectively. For comparison, the amounts adsorbed to nonporous silica, Aerosil 130, in the same solvents are also shown.^{19,29,30} The molecular weight dependence of the adsorbed amount for $M_w < 10^5$ in cyclohexane is similar, irrespective of the silica surface. In contrast, when $M_w > 355 \times 10^3$ the adsorbed amount depends strongly on the silica surface and is less than that for nonporous silica, where the amount adsorbed at the plateau is independent of the molecular weight. Such a negative deviation is clearly observed with

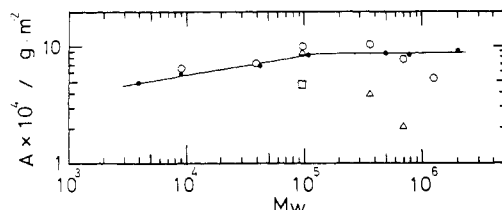


Figure 9. Double-logarithmic plots of the amounts adsorbed at the plateau in carbon tetrachloride at various silica surfaces against the weight-average molecular weight. The symbols are the same as in Figure 8. Since the respective amounts adsorbed for PS-9 and PS-38 are almost independent of the silica surface, the data are represented by the symbol \circ for MB-1300.

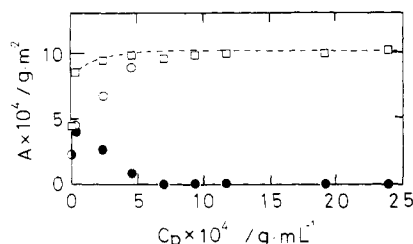


Figure 10. Adsorption isotherm of a binary mixture of PS-96 and PS-355 on the MB-1300 silica surface in carbon tetrachloride at 35 °C: (\square) mixture; (\bullet) PS-96 in mixture; (\circ) PS-355 in mixture. The dashed line indicates the adsorption isotherm of PS-355 on the MB-1300 silica surface.

a size ratio less than 2, and it increases with an increase in the molecular weight and in the order MB-1300 < MB-800 < MB-300.

On the other hand, for the molecular weight dependence of the adsorbed amount in carbon tetrachloride the trend is the same as for that in cyclohexane. The negative deviation from a curve fitted with the plot of the adsorbed amounts for the nonporous silica against the molecular weight is clearly observed when the size ratio is less than 2.

According to fractal analysis,^{31,32} the adsorbed amount per unit area decreases with an increase in the fractal dimension. Thus, the fractal dimension of the porous silicas is hardly different from that of the nonporous silica if the adsorbed amount on the porous silica is the same as that on the nonporous silica. When the adsorbed amount on the porous silicas is less than that on the nonporous silica, the fractal dimension of the porous silica is larger than that of the nonporous silica.

Isotherms of Competitive Adsorption. Figure 10 shows an adsorption isotherm of the mixture of PS-96 and PS-355 for the MB-1300 silica surface. The adsorption isotherm of the mixture is similar in shape to the high-affinity adsorption isotherm of the individual adsorption. The adsorption isotherm consists of the following three regions: (1) an initial steeply rising part where each component adsorbs completely with equal adsorbed amounts, (2) a region below $C_p = 0.045$ g/100 mL where PS-355 chains adsorb preferentially over PS-96 and only PS-96 chains remain in the supernatant, and (3) above $C_p = 0.07$ g/100 mL where only PS-355 chains adsorb and the adsorbed amount attains a plateau for both PS. This result suggests that the preferential adsorption is complete and is attributed to the slightly larger amounts adsorbed at the plateau for PS-355.

The dashed line in Figure 10 corresponds to the adsorption isotherm of PS-355 and is almost equal to the adsorption isotherm of the mixture. A similar trend was obtained for the adsorption of PS mixtures on the nonporous silica surface when the amounts adsorbed at the

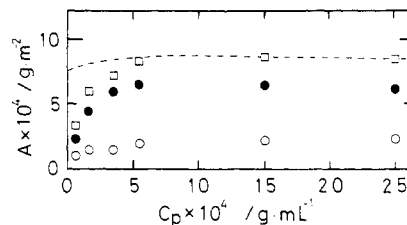


Figure 11. Adsorption isotherm of a binary mixture of PS-96 and PS-355 on the MB-800 silica surface in carbon tetrachloride at 35 °C. The symbols are the same as in Figure 10. The dashed line indicates the adsorption isotherm of PS-96 on the MB-800 silica surface.

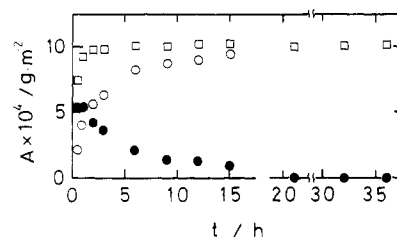


Figure 12. Plots of the total adsorbed amount (\square), adsorbed amount of PS-96 (\bullet), and adsorbed amount of PS-355 (\circ) as a function of the adsorption time, t , for the MB-1300 silica surface from a PS-96 and PS-355 mixture carbon tetrachloride solution. The initial added concentration is 0.075 g/100 mL for the respective PS samples.

plateau for the large PS is greater.³⁰ Furusawa et al.¹⁶ have reported that the isotherm for the binary mixtures, where both PS can penetrate into pores, has a much more rounded shape than that for the individual adsorption. The amount adsorbed at the plateau was equal to that for the individual adsorption. The significance of this discrepancy is not clear.

As seen from Figure 11, the adsorption isotherm of the mixture for the MB-800 is different in shape from that for MB-1300. The adsorption isotherm has a rounded shape isotherm, such as is often observed for adsorption of poly-disperse polymer samples. Only PS-96 adsorbs completely even at the lowest added concentration of each component (0.0125 g/100 mL), which corresponds to $C_p = 0.007$ g/100 mL. Below $C_p = 0.016$ g/100 mL all PS-96 adsorb and only PS-355 chains remain in the supernatant. Above $C_p = 0.016$ g/100 mL both PS chains remain in the supernatant, the total adsorbed amount increases with an increase in C_p and then attains a plateau. PS-96 chains adsorb more than PS-355 in the entire concentrations investigated, and the total amount adsorbed at the plateau is almost equal to the individual adsorption of PS-96, which is shown by a dashed line in Figure 11. In other words, the respective amounts adsorbed at the plateau are less than the individual adsorptions. This result shows that the available adsorption surface areas of the porous silicas are well used even for the competitive adsorption at the plateau.

Furusawa et al.¹⁶ also studied the similar system, and the adsorption isotherm for the binary mixture was different from ours: the apparent plateau adsorption was only observed, and its adsorbed amount was lower than the individual adsorption of the small PS.

Kinetics of Competitive Adsorption. Since Furusawa et al.¹⁶ have not investigated extensively kinetics of the competitive adsorption, we do not compare our results with theirs. Figure 12 shows plots of the adsorbed amounts of the mixture and each component in the mixture for the MB-1300 silica as a function of the adsorption time at the initial concentration of each PS sample, 0.075 g/100 mL,

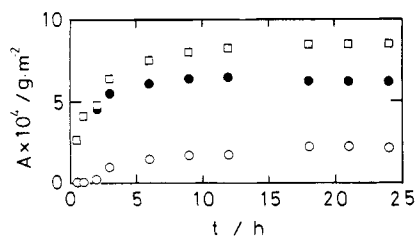


Figure 13. Plots of the total adsorbed amount (\square), adsorbed amount of PS-96 (\bullet), and adsorbed amount of PS-355 (\circ) as a function of adsorption time, t , for the MB-800 silica surface from a PS-96 and PS-355 mixture carbon tetrachloride solution. The initial added concentration is 0.05 g/100 mL for the respective PS samples.

where the adsorbed amount of each PS is in the plateau region for the adsorption isotherm of the mixture. From Figure 12, the total adsorbed amount is found to attain an apparent equilibrium state within 5 h, but each component does not attain its respective equilibrium state. During the initial 2 h the small PS adsorbs more than the large PS due to the difference in their diffusion coefficients. Beyond the interval of 2 h the reverse is observed, and true equilibrium is established in over 20 h.

Figure 13 displays plots of the amounts adsorbed for the mixture and the respective PS chains in the mixture for the MB-800 silica as a function of adsorption time from the initial concentration of each component, 0.05 g/100 mL, where the adsorbed amounts of the respective PS chains are well in the plateau region for the adsorption isotherm for the competitive adsorption. The initial adsorption time dependence is quite different from that for MB-1300. The kinetics lead to no apparent equilibrium. During the initial 2 h only the small PS adsorbs due to the large size ratio of the PS-96-MB-800 pair and the large diffusion coefficient of PS-96; later the large PS starts to adsorb, and finally the adsorbed amounts of the respective PS chains attain equilibrium.

Careful inspection of Figure 13 indicates that there are three steps in the adsorption kinetics for the large PS chains: the initial stage of less than 2 h (no adsorption), the middle adsorption time from 2 to 18 h ($A = 1.7 \times 10^{-4}$ g/m²), and the plateau region ($A = 2.3 \times 10^{-4}$ g/m²). A similar time dependence of the adsorbed amount was observed for the kinetics of the individual adsorption of PS-355 and MB-800 as shown in Figure 2. The kinetic study shows that the competitive adsorption on the porous silica surfaces attains equilibrium in less than a day. This is almost the same as for the individual adsorption.

Conclusions

The central result of this study is to show experimentally how a porous surface influences polymer adsorption in good and θ solvents. Kinetics and adsorption isotherms of individual and competitive adsorptions were studied in terms of the size ratio between the pore size to the polymer chain diameter. For the individual adsorption, measuring the amounts of PS adsorbed on the porous silica (size ratio ~ 2.0) at lower initial concentrations led to evidence for the existence of three stages in polymer adsorption kinetics: a steep rise of the adsorbed amount in the initial stage, a middle stage without an increase in adsorbed amounts, and the attainment of equilibrium in the final stage. For a size ratio > 1.5 , the initial stage of the adsorption is

dominated by polymer diffusion. Solvent power effects on kinetics are not evident at lower initial concentrations but are important at higher initial concentrations. Moreover, it was found that the molecular weight dependence of the amount adsorbed at the plateau differs clearly from that for the nonporous silica surface above $M_w \sim 100 \times 10^3$.

The size ratio also influences the competitive adsorption. When the size ratio for both PS chains is larger than 2, the competitive adsorption is governed by the preferential adsorption of the large PS chains and this behavior is the same as that for the nonporous silica surface. By contrast, when the size ratio for the large PS is less than 2 and the size ratio for the small PS is larger than 2, the adsorbed amount of the small PS is larger.

References and Notes

- (1) Takahashi, A.; Kawaguchi, M. *Adv. Polym. Sci.* **1982**, *46*, 1.
- (2) Cohen Stuart, M. A.; Cosgrove, T.; Vincent, B. *Adv. Colloid Interface Sci.* **1986**, *24*, 143.
- (3) Howard, G. J. In *Interfacial Phenomena in Apolar Media*; Eicke, H.-F., Parfitt, G. D., Eds.; Dekker: New York, 1987; p 281.
- (4) de Gennes, P.-G. *Adv. Colloid Interface Sci.* **1987**, *27*, 189.
- (5) Fleer, G. J.; Scheutjens, J. M. H. M.; Cohen Stuart, M. A. *Colloids Surf.* **1988**, *31*, 1.
- (6) Stromberg, R. R.; Tutas, D. J.; Passaglia, E. *J. Phys. Chem.* **1965**, *69*, 3955.
- (7) Takahashi, A.; Kawaguchi, M.; Hirota, H.; Kato, T. *Macromolecules* **1980**, *13*, 884.
- (8) Kawaguchi, M.; Hayakawa, K.; Takahashi, A. *Macromolecules* **1983**, *16*, 631.
- (9) Penners, G.; Priel, Z.; Silberberg, A. *J. Colloid Interface Sci.* **1981**, *80*, 437.
- (10) Aizenbud, B.; Volterra, V.; Priel, Z. *J. Colloid Interface Sci.* **1985**, *103*, 133.
- (11) Pefferkorn, E.; Carroy, A.; Varoqui, R. *J. Polym. Sci., Polym. Phys. Ed.* **1985**, *23*, 1997.
- (12) Loulergue, J. C.; Levy, Y.; Allain, C. *Macromolecules* **1985**, *18*, 306.
- (13) Pefferkorn, E.; Carroy, A.; Varoqui, R. *Macromolecules* **1985**, *18*, 2252.
- (14) Pefferkorn, E.; Haouam, A.; Varoqui, R. *Macromolecules* **1988**, *21*, 2111.
- (15) Cohen-Addad, J.-P.; Huchot, P.; Jost, P.; Pouchelon, A. *Polymer* **1989**, *30*, 143.
- (16) Furusawa, K.; Yamashita, K.; Konno, K. *J. Colloid Interface Sci.* **1982**, *86*, 35.
- (17) Kawaguchi, M.; Arai, T. *Macromolecules* **1991**, *24*, 889.
- (18) Berry, G. C. *J. Chem. Phys.* **1966**, *44*, 4550; **1967**, *46*, 1338.
- (19) Kawaguchi, M.; Chikazawa, M.; Takahashi, A. *Macromolecules* **1989**, *22*, 2195.
- (20) Cohen Stuart, M. A.; Fleer, G. J.; Scheutjens, J. M. H. M. *J. Colloid Interface Sci.* **1984**, *97*, 515, 526.
- (21) Kawaguchi, M.; Hada, T.; Takahashi, A. *Macromolecules* **1989**, *22*, 4045.
- (22) Kawaguchi, M. In *Space-Time Organization in Macromolecules Fluids*; Tanaka, F., Doi, M., Ohta, T., Eds.; Springer-Verlag: Berlin and Heidelberg, 1989; p 162.
- (23) Van der Beek, G. P.; Cohen Stuart, M. A.; Fleer, G. J.; Hofman, J. E. *Langmuir* **1989**, *5*, 1980.
- (24) Glöckner, G. *Polymer Characterization by Liquid Chromatography*; Elsevier: Amsterdam, The Netherlands, 1987.
- (25) Bishop, M. T.; Langley, K. H.; Karasz, F. E. *Phys. Rev. Lett.* **1986**, *57*, 1741.
- (26) Bishop, M. T.; Langley, K. H.; Karasz, F. E. *Macromolecules* **1989**, *22*, 1231.
- (27) Easwar, N.; Langley, K. H.; Karasz, F. E. *Macromolecules* **1990**, *23*, 738.
- (28) Akcasu, A. Z.; Han, C. *Macromolecules* **1979**, *12*, 276.
- (29) Kawaguchi, M.; Hayakawa, K.; Takahashi, A. *Polym. J.* **1980**, *12*, 265.
- (30) Kawaguchi, M.; Maeda, K.; Kato, T.; Takahashi, A. *Macromolecules* **1984**, *17*, 1666.
- (31) Mandelbrot, B. B. *The Fractal Geometry of Nature*; Freeman: San Francisco, CA, 1982.
- (32) Farin, D.; Avnir, D. *Colloids Surf.* **1989**, *37*, 155.

Registry No. PS, 9003-53-6; silica, 7631-86-9.